



PII S0016-7037(00)00559-7

Oceanographic considerations for the application of the alkenone-based paleotemperature $U_{37}^{K'}$ index in the Gulf of California

MIGUEL A. GOÑI,^{1,*} DAVID M. HARTZ,² ROBERT C. THUNELL,¹ and ERIC TAPPA¹¹Department of Geological Sciences, University of South Carolina, Columbia, SC 29208, USA²Texaco Brazil Suite 1600, 3040 Post Oak Blvd, Houston, TX 77056, USA

(Received August 2, 1999; accepted in revised form October 11, 2000)

Abstract—Alkenone concentrations were determined in sediment trap samples and surficial sediments collected from Guaymas Basin (Gulf of California) to investigate the factors that control the relationship between the $U_{37}^{K'}$ index and SST. The results from the sediment trap study reveal a positive correlation ($r^2 = 0.5$) between alkenone fluxes and satellite AVHRR sea surface temperature (SST) and a strong correlation ($r^2 = 0.9$) between $U_{37}^{K'}$ and SST over an annual temperature range of 20°C. Although SST and $U_{37}^{K'}$ are tightly coupled throughout two upwelling seasons, the relationship deviates from the expression developed by Prahl et al. (1988) at temperatures higher than 26°C. The possible reasons for this deviation are varied but include the observed changes in the coccolithophore species assemblage and the evolution of the thermocline during periods of high SST. The seasonal pattern of alkenone fluxes (higher fluxes during warm periods) observed throughout the 1996 to 1997 study period causes a “bias” in the annually averaged $U_{37}^{K'}$ record, resulting in temperature estimates that are ~1°C higher than the annual AVHRR SST average. Furthermore, the $U_{37}^{K'}$ ratios obtained from core-top sediments indicate an additional ~2°C “warm bias” in the sedimentary record that may be related to the lateral inputs of alkenones from other regions of the Gulf. These results highlight the importance of oceanographic processes in determining the alkenone temperature signal that is preserved in sediments. After accounting for such effects, $U_{37}^{K'}$ ratios from a box core were used to reconstruct a SST record extending back to the 18th century for the Guaymas Basin. These results indicate a steady 2°C warming of the surface waters of the Gulf from early 1700s to the 1950s, followed by a rapid apparent 1°C cooling between the 1950s and the 1980s. Copyright © 2001 Elsevier Science Ltd

1. INTRODUCTION

Haptophyte algae, including the coccolithophores *Emiliania huxleyi* and *Gephyrocapsa oceanica*, are major producers of a suite of long chain unsaturated ketones, alkenones (Volkman et al., 1980; Marlowe et al., 1984). These algae, which are ubiquitous throughout the world's oceans (e.g., Marlowe et al., 1990), alter the degree of unsaturation of individual ketones as a physiological response to changes in the temperature of the surrounding water (Prahl and Wakeham, 1987; Prahl et al., 1988). Two parameters, the $U_{37}^{K'}$ and $U_{37}^{K''}$ unsaturation indexes, have been developed to summarize the changes in the proportions of the commonly measured C_{37} ketones. Several studies have shown that the $U_{37}^{K'}$ index, in particular, is relatively insensitive to diagenesis (e.g., Prahl et al., 1989; Sikes et al., 1991; Rontani et al., 1997; Teece et al., 1998), although new studies by Hoefs et al. (1998) and by Gong and Hollander (1999) suggest that differences in the degradation of alkenones under oxic and anoxic conditions may affect the temperature signature preserved in sediments. Nevertheless, $U_{37}^{K'}$ values obtained from marine sediments have been used to reconstruct sea surface temperatures (SST) in many regions of the ocean (recent studies include Ikehara et al., 1997; Pelejero and Grimalt, 1997; Rosell-Mele et al., 1997; Sikes et al., 1997; Herbert et al., 1998; Muller et al., 1998; Sonzogni et al., 1998; Ternois et al., 1998; Thomsen et al., 1998; Villanueva et al., 1998; Pelejero et al., 1999).

In paleoceanographic studies, variations in $U_{37}^{K'}$ have been found to correlate well with other proxies of temperature such as the $\delta^{18}O$ of foraminiferal calcite (Brassell et al., 1986; Sikes and Keigwin, 1994) and radiolarian species assemblages (Prahl et al., 1995). However, as evidenced by the discussions at the recent NSF-sponsored workshop on alkenone-based paleoceanographic indicators, questions still remain regarding the accuracy of the alkenone approach for SSTs reconstructions (Eglinton et al., 2000). Much of the debate has focused on the validity of using a single expression that relates the alkenone unsaturation index and growth temperature of haptophyte algae to estimate past temperatures of the surface ocean. Culture studies have shown that different species and strains of haptophyte algae can yield variable linear and nonlinear relationships between $U_{37}^{K'}$ and temperature (e.g., Volkman et al., 1995; Conte et al., 1998), which deviate from the original expression developed for *E. huxleyi* (Prahl et al., 1988). Recent culture work by Epstein and co-workers also suggests that nutrient concentrations may affect the $U_{37}^{K'}$ ratio of *E. huxleyi* (Epstein et al., 1998). Oceanographic studies indicate that the $U_{37}^{K'}$ ratios of marine particles can be biased towards the season and depth of highest haptophyte productivity (e.g., Sikes et al., 1991; Conte et al., 1992; Prahl et al., 1993; Ohkouchi et al., 1999), and are affected by species composition (e.g., Sikes and Volkman, 1993; Prahl et al., 1995) and lateral alkenone inputs (e.g., Thomsen et al., 1998). These processes, which are most pronounced in upwelling and continental margin regions of the ocean, have the potential to drastically alter the relationship between the $U_{37}^{K'}$ index and growth temperature recorded in

* Author to whom correspondence should be addressed: goni@geol.sc.edu).

marine sediments and, thus, hamper the use of this proxy for SST reconstructions.

Despite these potential problems, several studies (Rosell-Mele et al., 1995b; Sonzogni et al., 1997; Muller et al., 1998; Herbert et al., 1998) have shown a remarkable linear relationship between the $U_{37}^{K'}$ index recorded in surface sediments and the annual mean SSTs (Levitus, 1994). Notably, the Muller et al. relationship (1998), which is virtually identical to that originally developed by Prah1 and co-workers (Prah1 and Wakeham, 1987; Prah1 et al., 1988), is linear over a temperature range of 0 to 27°C and describes data from different regions of the global ocean. The agreement between mean annual SSTs and $U_{37}^{K'}$ ratios evident in these core-top calibrations is partially due to the fact that most of the data used in these studies are derived from open ocean sites, where seasonal and inter-annual variability (in both haptophyte productivity and SSTs) tends to be low. Mixing of surficial sediments by bioturbation further smoothes any temporal differences at these locations. Surprisingly, however, the agreement between the core-top calibrations and the Prah1 et al., (1988) equation is also good in some upwelling sites that exhibit large seasonal contrasts and high sedimentation rates (e.g. Herbert et al., 1998). The question still remains of why $U_{37}^{K'}$, a biologic parameter with all its intrinsic variance and heterogeneity, appears to be such a robust indicator of past SSTs. Addressing this controversy is critical for the application of alkenones in paleoceanographic studies and requires a better understanding of the processes that control the generation and transfer of the $U_{37}^{K'}$ signal in the water column and its preservation in sedimentary record.

In this study, we use modern day data on SST, alkenone export from the euphotic zone, and alkenone accumulation in surficial sediments, to investigate the processes that control how the alkenone-based temperature signatures are preserved in the sedimentary record. Furthermore, to evaluate the significance of these processes on the reconstruction of paleo SST, we contrast our results with those derived from the application of the widely utilized Prah1 et al. (1988) $U_{37}^{K'}$ equation. We report $U_{37}^{K'}$ values derived from alkenone analyses of sediment trap materials collected in Guaymas Basin, Gulf of California, over a 21-month period. The unsaturation index values are compared with satellite-derived Advanced Very High Resolution Radiometer (AVHRR) sea surface temperatures for the same time interval. In addition, we report alkenone compositions for box core sediments collected within the oxygen minimum zone in the basin that approximately expand the last 300 years. Several unique aspects characterize this study. One is the large temperature range observed in the surface waters at the Guaymas site (15–32°C). We also were able to acquire synchronous measurements of SSTs (by AVHRR) and alkenone export from the euphotic zone (by sediment traps), and compare them to records of thermocline evolution and coccolithophore fluxes. Finally, the varved nature of the underlying sediments made it possible to contrast water column and sedimentary fluxes in the absence of bioturbation. These characteristics allow us to (1) assess the response of haptophyte algae to rapid temperature changes; (2) investigate the effects of haptophyte seasonal productivity on the annually averaged $U_{37}^{K'}$ signal reaching the sediments; and (3) shed additional light on the processes by which this temperature proxy is incorporated

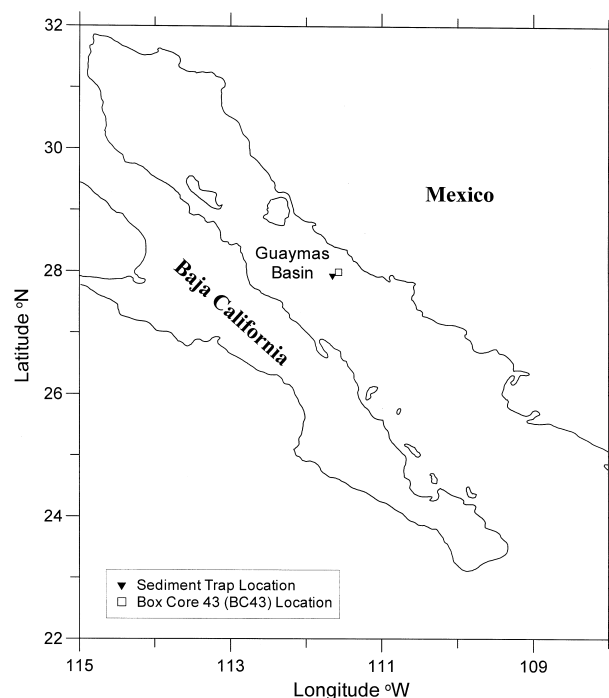


Fig. 1. Map showing the location of the sediment trap and box core (BC-43) used in this study.

into the sedimentary record. We approach the latter objective as an open-ended question that should be a critical component of future work in this and other areas of the ocean.

2. REGIONAL SETTING

2.1. Hydrography and Productivity

The Gulf of California is a large evaporative basin divided by silled basins that deepen towards the south (Alvarez-Borrego and Schwartlose, 1979). Guaymas Basin is one of the larger basins located in the central part of the Gulf (Fig. 1). The wind patterns within the gulf reverse seasonally in response to changes in the location of the large-scale pressure fields (Badan-Dangon et al., 1991). The seasonal evolution of the thermocline in Guaymas Basin under this monsoon regime is summarized in Figure 2. During the winter months, strong northwesterly winds blow down the gulf's axis inducing extensive upwelling and resulting in surface water temperatures as low as 15°C (Fig. 2; Robinson, 1973; Thunell, 1998). During the summer months winds reverse and become southeasterly up the gulf's axis, leading to the shut down of upwelling. The combination of decreased upwelling and high insolation causes a marked heating of the upper water column and the development of strong thermal stratification. Under these conditions, temperatures at the sea surface exceed 30°C in Guaymas during the summer months (Fig. 2).

The monsoon climate in the Gulf of California leads to marked seasonal changes in productivity and biogenic sediment fluxes through the water column (e.g., Alvarez-Borrego and Lara-Lara, 1991; Thunell, 1998). In general, pigment concentrations in surface waters are negatively correlated with SST (Thunell et al., 1996; Thunell, 1998). During the upwelling period (November–March), surface waters within the gulf exhibit high levels of primary productivity that are 2 to 3 times higher than those observed within the open Pacific at similar latitudes (Zeitzschel, 1969). Conversely, primary production is low during the rainy period (May–September) when stratified conditions prevail (Thunell, 1998). Analyses of sediment trap materials (Thunell et al., 1996; Thunell, 1998) reveal that diatom cell and biogenic opal fluxes correlate well with pigment concentrations and are highest

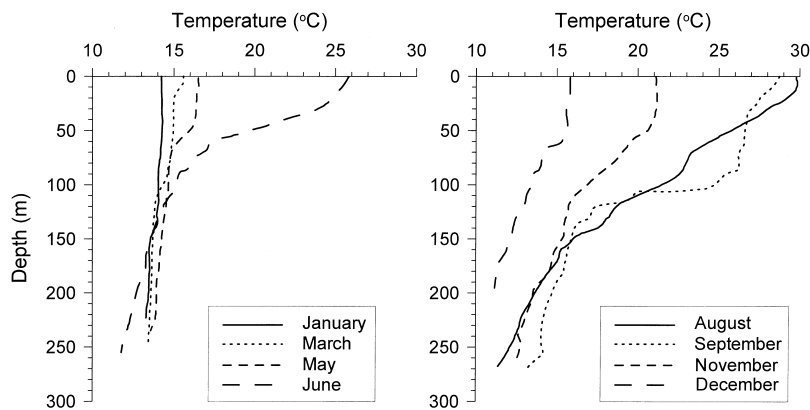


Fig. 2. Temperature profiles of the upper water column in Guaymas Basin. Data represent monthly averages measured by Robinson, 1973.

during the early stages of upwelling (typically November–January). In contrast, the fluxes of coccolithophores and calcium carbonate are not highly correlated with pigment concentration. In fact, coccolith fluxes show distinct peaks during periods of upper water column stratification, both at the beginning and at the end of the summer (Thunell et al., 1996; Ziveri and Thunell, 2000). The species compositions of the sediment trap samples collected during 1992 reveal that the initial peak in coccolith flux (during May and June) is composed primarily of *E. huxleyi*, whereas the latter flux peak (during September) is due primarily to *Gephyrocapsa oceanica* (Ziveri and Thunell, 2000).

2.2. Depositional Environment

Pacific Intermediate Water, which flows into the Gulf at depths below 500 meters, exhibits a strong oxygen minimum zone (OMZ) between 500 to 1000 meters (Calvert, 1966). At these depths, biologic activity in the sediments of Guaymas basin and other areas of the Gulf is inhibited. Seasonal variations in the composition of sediments delivered to the seafloor, combined with this lack of bioturbation, allow varved sediments to accumulate within this depth range (Baumgartner et al., 1991; Thunell et al., 1993; Thunell, 1998). Each varve is a sedimentary couplet of a light and a dark lamina. The light laminae consist primarily of opal deposited during the high productivity season, which occurs from late fall through the spring (Thunell, 1998). The dark layers are rich in lithogenic material that is deposited during the summer months when winds are weaker and from the south (Baumgartner et al., 1991; Thunell et al., 1993).

3. SAMPLE COLLECTION

3.1. Sediment Trap Samples

Sediment trap samples used in the present study were collected as part of a long-term program designed to study seasonal to interannual variability in sediment fluxes within the Guaymas Basin (27°53'N, 111°40'W) (Fig. 1) (Thunell, 1998). The sediment trap was initially deployed in August 1990 at a depth of approximately 500 m from the sea surface and 200 m off the bottom within the OMZ. Since its deployment, materials settling through the water column were collected continuously at two week intervals for eight years. A buffered sodium azide solution was placed within each trap cup before deployment to prevent biological activity after sample collection. After recovery of the trap, each cup was sealed and refrigerated prior to analysis. In this study, we analyzed one bi-weekly trap sample per month for the period from January 1996 to September 1997.

3.2. Sea Surface Temperature Data

A record of SST for the Guaymas Basin sediment trap location was determined for the study period by using weekly composites of AVHRR data. AVHRR data used in this study were collected daily and weekly averages were estimated for each sample collection period using all available daytime data from a 18 Km × 18 Km pixel area surrounding the study site (for more details see Thunell, 1998).

3.3. Sediment Samples

Surface sediments were collected by a box core during a cruise in June 1990 aboard the R/V Atlantis II. Box core 43 (BC-43) (Fig. 1) was collected at depth of 655 m along the eastern flank of the Guaymas basin (27°54.05'N, 111°39.43'W) and displayed varved sediments throughout. For this study a six-inch diameter subcore was taken, sealed and stored unaltered in a refrigerated room. One half of the 31 cm long sub-core was sampled continuously at 0.5-cm intervals. The excess ²¹⁰Pb profile of this core showed a smooth exponential profile that indicated an average sedimentation rate of 1.16 mm/yr (Pride, 1997; Cutshall et al., 1983).

4. ANALYTICAL METHODS

4.1. Alkenone Extraction

A slightly modified procedure of the method developed by Rosell–Melé and co-workers (Rosell–Mele et al., 1995a) was used for the extraction and subsequent preparation of alkenones (see Hartz, 1998 for details). Briefly, known amounts of oven-dried (at 50°C), finely ground sediment trap materials and box core sediments were solvent extracted in triplicate with dichloromethane/methanol (3:1) by using a Benchmate™ II Workstation. Before extraction a known amount of hexatriacontane was added as a recovery standard. A sonication step was used to aid the extraction process. After extraction the extracts were transferred to a new tube and dried by using a Turbovap LV (Zymark Corp., Hopkinton MA) at 40°C under a nitrogen stream. The dried extracts were redissolved in dichloromethane and loaded onto preconditioned SPE columns (Accubond, 3 mL–200 mg silica adsorbant, J & W Scientific) for clean-up.

Each column was conditioned with 3 mL of methanol and 3 mL of dichloromethane in succession. A mixture of dichloromethane/1% methanol was used to elute the alkenone-containing solution, which was dried in preparation for gas chromatographic analysis.

4.2. Gas Chromatographic (GC) Analysis

Before GC analysis, 30 μ L of Regisil, BSTFA + 1% TMCS (Regis Technologies Inc.) and 50 μ L of ethyl acetate were added to a portion of the extract to silylate acids and alcohols. The silylation reaction was carried out at room temperature in sealed vials placed in a desiccator overnight. After derivatization, the dissolved extracts were evaporated under a gentle nitrogen stream and redissolved in 25 to 100 μ L of dichloromethane for GC analysis. Gas chromatographic analysis was performed with a Hewlett–Packard 6890 GC equipped with on-column injector, flame ionization detection and electronic pressure control. Separation of the alkenones was achieved by using a 60 m DB-1 GC column (J & W Scientific) with 0.32 mm internal diameter and 0.25 μ m film thickness and a constant He flow of 1.3 mL/min. Alkenone concentrations were quantified based on the amount of hexatriacontane detected in the GC trace and assuming a similar response factor for the FID detection of both alkenones. The identities of di- and tri-unsaturated C₃₇ methyl ketones (37:2 Me and 37:3 Me, respectively) were verified by co-injection of synthetic standards provided by A. Rosell–Mele and examination of electron ionization mass spectra obtained with a HP 5970 GC-MS. The tetra-unsaturated alkenone (37:4 Me) was undetected in these samples and was, therefore, excluded from the calculation. The unsaturation index was calculated by using the concentrations of the C₃₇ ketones according to $U_{37}^{K'} = [37:2 \text{ Me}] / [37:2 \text{ Me} + 37:3 \text{ Me}]$ (Prahl and Wakeham, 1987). Based on replicate analyses, the average standard deviation for individual alkenone concentrations ranges from 10% to 30% of the measured value with the higher errors occurring in samples with low alkenone content. The average variability associated with the $U_{37}^{K'}$ ratio is ± 0.01 , which corresponds to a variance in the estimated temperature of ca. $\pm 0.3^\circ\text{C}$.

4.3. Organic Carbon Analyses

Organic carbon (%OC) contents were determined for sediment trap and sediment samples using a Perkin–Elmer 2400 Elemental Analyzer and following the procedure of Froelich (1980). Briefly, samples were pre-weighed, acidified with 100% phosphoric acid to remove carbonates and recovered on precombusted filters, which were run in the elemental analyzer. The reproducibility of this approach is better than 0.05 weight %. Losses of organic matter by leaching during the acidification process are possible using this procedure, leading to potential underestimation of %OC. On the other hand, alternative approaches that involve sample pretreatment with acid vapors (e.g., Hedges and Stern, 1984), and/or acid liquids (e.g., Cowie and Hedges, 1991) can result in incomplete removal of inorganic carbonate and an overestimation of %OC (e.g., Weliky et al., 1983). To assess the effect of our analytical technique, we analyzed a selected number of sediment trap samples by other methods, including in situ vapor and liquid phase acidification,

Table 1. Comparison of weight %OC values obtained from Guaymas basin sediment trap samples by different analytical methods.

Analytical method	Oct-94 Sample %OC \pm SD	Mar-95 Sample %OC \pm SD
Glass fiber filter ^a	4.35 \pm 0.04	5.20 \pm 0.05
By difference (%TC–%IC) ^b	4.46 \pm 0.25	5.63 \pm 0.10
Acid vapor treatment ^c	4.93 \pm 0.05	5.81 \pm 0.14
Acid vapor + liquid treatment ^d	5.02 \pm 0.22	5.85 \pm n.m.

Analytical methods: ^a Acidification with phosphoric acid followed by filtration (Froelich, 1980); ^b Determination of %OC by the difference between Total Carbon (%TC) and Inorganic Carbon (%IC) (e.g., Goñi et al., 1998); ^c Removal of carbonate from sample in silver boat by exposure to acid fumes (e.g., Hedges and Stern, 1984); ^d Removal of carbonate from sample in silver boats by acid fumes followed by treatment with 1N HCl liquid (e.g., Cowie and Hedges, 1991). Captions: SD, standard deviation; n.m., not measured.

and determination of %OC by the difference between total carbon and total inorganic carbon (e.g., Goñi et al., 1998). The data in Table 1 show that all methods yield similar results, although the filtering method gives %OC values that are up to 10% lower than the those obtained by the other methods. It is beyond the scope of this paper to discuss the reasons for the observed differences in %OC. Nevertheless, this comparison suggests that the concentration and flux data presented below should be taken as conservative estimates.

5. RESULTS

5.1. AVHRR Sea Surface Temperatures

A multi-year record of weekly composite AVHRR SST estimates illustrates the upwelling-driven periodicity in the temperature signal of the upper water column at Guaymas Basin (Fig. 3). Overall, the satellite-derived SST data are consistent with the annual range previously reported for the Gulf of California (Zeitzschel, 1969) and the monthly means reported

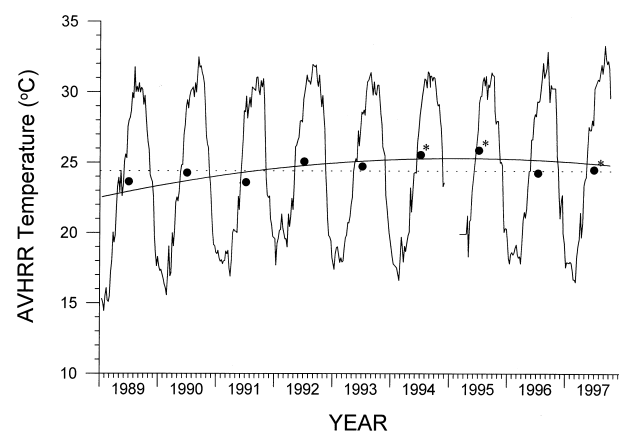


Fig. 3. Multi-year record of sea surface temperature obtained by Advanced Very High Resolution Radiometer (AVHRR) for Guaymas Basin. Annual mean temperatures are illustrated with a (●); * indicates annual means that contain an incomplete record. The curve represents a nonlinear fit of the whole temperature record. The dotted line delineates the average AVHRR temperature for the whole period (1989–1997).

Table 2. Compositions and characteristics of sediment trap samples.

Dates of Trap Deployment		AVHRR T (°C)	Mass Flux (g/m ² /d)	%OC (wt.%)	ΣAlk (μg/g sed)	U ₃₇ ^{K'}
(trap open)	(trap close)					
14-Jan-96	28-Jan-96	18.4	0.303	4.61	7.97	0.69
11-Feb-96	25-Feb-96	19.0	0.626	4.31	7.77	0.75
10-Mar-96	24-Mar-96	18.1	0.323	5.27	7.76	0.62
10-Apr-96	24-Apr-96	21.3	0.259	5.80	7.72	0.80
8-May-96	22-May-96	24.5	0.387	5.17	10.56	0.84
19-Jun-96	3-Jul-96	28.8	0.618	4.69	16.37	0.89
17-Jul-96	31-Jul-96	30.7	0.311	5.14	10.03	0.94
28-Aug-96	11-Sep-96	32.4	0.400	5.50	25.16	0.97
29-Sep-96	13-Oct-96	30.3	0.505	5.55	19.88	0.98
13-Oct-96	27-Oct-96	29.4	0.303	5.61	16.19	0.98
10-Nov-96	24-Nov-96	22.5	0.868	3.11	11.75	0.87
8-Dec-96	22-Dec-96	20.1	0.490	3.47	9.75	0.72
5-Jan-97	19-Jan-97	17.8	0.465	3.44	14.61	0.65
2-Feb-97	16-Feb-97	17.7	0.366	4.92	11.38	0.63
2-Mar-97	16-Mar-97	17.1	0.309	4.86	10.39	0.64
6-Apr-97	20-Apr-97	20.4	0.638	5.80	10.74	0.71
18-May-97	1-Jun-97	27.1	1.178	3.82	6.81	0.86
15-Jun-97	29-Jun-97	28.6	0.410	5.85	23.30	0.92
13-Jul-97	27-Jul-97	30.9	0.573	4.71	24.88	0.97
10-Aug-97	24-Aug-97	31.7	0.637	4.87	19.96	0.98
21-Sep-97	4-Oct-97	31.3	0.780	5.13	15.38	0.97

Captions: AVHRR T, composite sea surface temperature estimated from advance very high resolution radiometer data for the periods of sample collection; Mass Flux, estimated flux of total mass (dry weight) collected during each deployment period; ΣAlk, total alkenone concentrations (sum [37:3 Me] and [37:2 Me] concentrations); U₃₇^{K'}, alkenone unsaturation index.

by Robinson (1973; Fig. 2). It is notable that both the summer and winter temperatures measured by the satellite during 1989 to 1997 are 1 to 2°C higher than the values plotted in Figure 2, which were obtained from hydrocasts. There are several reasons that can account for these contrasts including differences in what is considered “surface” in both data sets (millimeters for AVHRR vs. meters for hydrocasts). Furthermore, these differences may also be indicative of actual interannual variations in the hydrography and climate of the region. For example, there are clear differences in the mean, minimum, and maximum SSTs within the AVHRR data plotted in Figure 3. These interannual differences are related to El Niño–Southern Oscillation (ENSO). El Niño conditions existed for much of 1990 to 1995 (Fig. 3; Thunell, 1998). During the period covered by this sediment trap study (1996–1997), the lowest SSTs (17 to 18°C) were measured during the winter months (January–March) of both years (Table 2; Fig. 4). The highest temperatures (30–32°C) were measured during the summer months (July–September). In both years, the marked warming of the surface water began in April, whereas surface cooling started in October (the end and the beginning of upwelling periods, respectively).

5.2. Sediment Trap Alkenone Concentrations and U₃₇^{K'} Values

The concentrations for the 37:2 Me and 37:3 Me alkenones in the sediment trap particles range from 4.8 to 116 and 0.34 to 47.0 μg/g sediment, respectively (Table 2). The concentrations of the 37:3 Me alkenone are lower than those of 37:2 Me in all trap samples as expected from the overall high surface water temperatures in the Gulf. The seasonal trends in the carbon-normalized concentrations of alkenones (ΣAlk) from sinking

particles are illustrated in Figure 4a. Overall, there is a weak correlation ($r^2 = 0.3$) between ΣAlk concentrations and SST during the two years of the study. Sinking particles display low alkenone contents (150–200 μg/g OC) during the winter upwelling months (January–March), whereas high ΣAlk values (350–550 μg/g OC) coincide with periods of high SST and water column stratification (June–October). Clearly, multiple factors can affect the ΣAlk concentrations of sinking particles, including dilution by other biogenic (e.g., diatoms) and lithogenic (aeolian dust) organic carbon sources. Furthermore, the ΣAlk/OC ratios of coccolithophore-derived materials can be modified through the seasonal cycle due to variations in the species composition of haptophyte algae, changes in physiological state of alkenone producers, and post-production diagenetic alterations in the water column. Hence, it is difficult to relate carbon-normalized ΣAlk concentrations to haptophyte primary productivity. Nevertheless, the general trend illustrated in Figure 4a indicates that elevated coccolithophore production tends to occur during the post-upwelling (warmer SST) periods.

Low U₃₇^{K'} ratios (≤ 0.65) were measured during March of 1996 and January to March of 1997 (Table 2). High values (> 0.95) were obtained from September to late October of 1996 and from late July to late September of 1997. Unlike the trend in ΣAlk concentrations, the changes in U₃₇^{K'} closely follows the seasonal cycle of surface water temperatures (Fig. 4b). The high correlation ($r^2 = 0.9$) between these two independent data sets indicates an almost immediate response of the haptophyte phytoplankton community to changes in SST and a rapid transfer of the signal to the sediment traps 500 m below the surface. Based on these observations, the ratios of individual alkenones in sinking particles from the Gulf of California appear to be independent of haptophyte production and com-

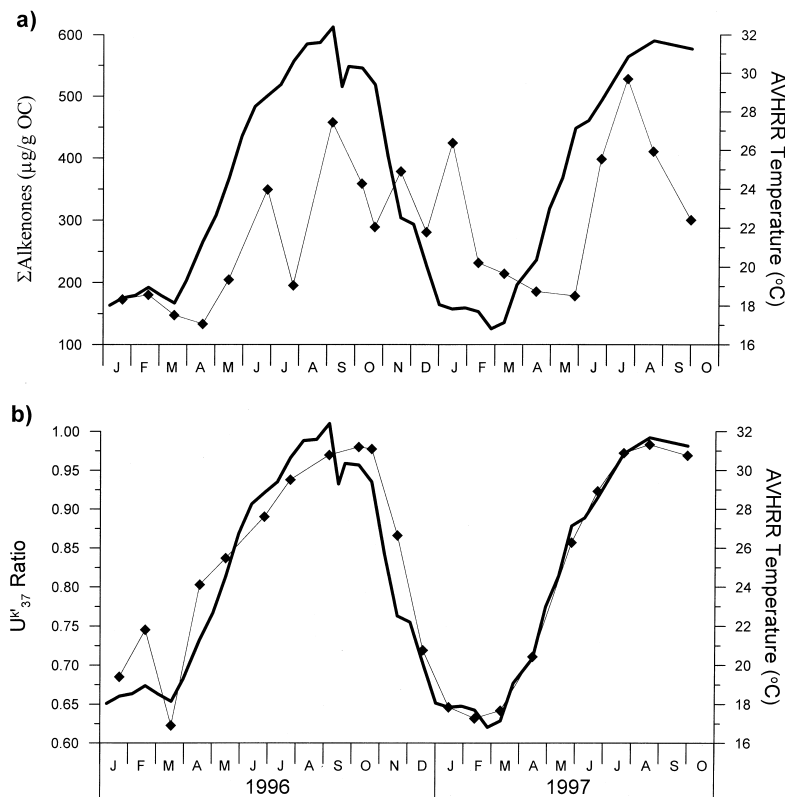


Fig. 4. Plot of a) carbon-normalized total alkenone (ΣAlk) concentrations and b) $U_{37}^{K'}$ ratios of sinking particles collected bi-weekly by the sediment trap in Guaymas Basin. The thick line represents the temperature changes of the sea surface as measured by AVHRR.

position, and thus, have the potential to accurately track temperature changes in the upper water column.

5.3. Box Core (BC-43) Alkenone Concentrations and $U_{37}^{K'}$ Values

Given the sedimentation rate for this core (1.16 mm/yr; Pride, 1997) and the 0.5 cm sampling increments, the average temporal resolution of each sample is approximately four years. Based on these data, BC-43 covers a time period from mid 1990 to ca. 1727 and encompasses approximately 260 yr of deposition (Table 3). The two major C_{37} ketones, 37:2 Me and 37:3 Me, were measured in appreciable concentrations throughout the box core. As was the case with the sediment trap samples, the 37:4 Me alkenone was not detected, reflecting the generally high temperatures in the Gulf. ΣAlk concentrations range from ca. 6 to 28 $\mu\text{g/g}$, averaging 13 $\mu\text{g/g}$ sediment for the whole core (Table 2). Both the sediment- (Table 2) and carbon-normalized ΣAlk concentrations (Fig. 5) display a slight downcore trend of decreasing values with depth with several marked deviations. Large fluctuations in the carbon-normalized ΣAlk concentrations are evident in the top of the core, with values ranging from 700 $\mu\text{g/g OC}$ to 200 $\mu\text{g/g OC}$ within the top 100 mm. Low values (200–300 $\mu\text{g/g OC}$) are observed between 100 and 150 mm and between 250 and 300 mm (with the exception of the peak at ~ 275 mm), whereas intermediate values (200–500 $\mu\text{g/g OC}$) are measured between 150 and 250 mm. Overall, the ranges in carbon-normalized alkenone content displayed by the sediments are comparable to those measured in the sediment trap samples (Fig. 4a). Such similarity argues

against a marked preferential decay and preservation of C_{37} alkenones relative to bulk organic matter. The variations in the ΣAlk concentrations along this core likely reflect historical changes in the relative contribution of haptophyte production to the organic matter preserved in sediments.

The $U_{37}^{K'}$ ratios of BC-43 sediments (Table 2) average 0.90 for the whole core and range from a minimum of 0.83 (27.0–27.5 cm interval) to a maximum of 0.95 (14.0–14.5 cm interval). There is a general downcore decrease in $U_{37}^{K'}$ ratios from values >0.90 at the top to values approaching 0.85 near the bottom (Fig. 5). As was the case for the sediment trap samples, there is no significant covariance between the $U_{37}^{K'}$ ratios and the ΣAlk concentrations.

6. DISCUSSION

6.1. $U_{37}^{K'}$ Index and Measured Sea Surface Temperature Relationship

The details of the relationship between the $U_{37}^{K'}$ ratios of sinking particles and the satellite-derived SST (Fig. 4b) are evident in Figure 6. The correlation between $U_{37}^{K'}$ and SST follows the linear equation of Prahl and co-workers ($U_{37}^{K'} = 0.034T + 0.039$; Prahl, 1988) in the lower range of the temperature record (17–26°C). In contrast, samples collected during periods of elevated temperatures (26–32°C) display $U_{37}^{K'}$ values that deviate significantly from the Prahl et al. relationship, plotting instead in a region defined by the expression of Volkman and co-workers ($U_{37}^{K'} = 0.049T - 0.520$; Volkman, 1995). Thus, despite the strong covariance between $U_{37}^{K'}$ and SST evident from Figure 4b, it is clear that the full range of

Table 3. Compositions of box core sediment samples.

Depth interval (cm)	Age ^a (yrs)	Deposition date ^b	%OC (wt.%)	ΣAlk (μg/g sed)	U ₃₇ ^{K'}
0–0.5	2	1988	4.71	16.14	0.90
0.5–1.0	6	1984	4.20	17.38	0.90
1.0–1.5	11	1979	4.17	16.79	0.90
1.5–2.0	15	1975	4.30	17.14	0.90
2.0–2.5	19	1971	4.03	8.87	0.90
2.5–3.0	24	1966	3.96	16.83	0.91
3.0–3.5	28	1962	3.92	15.66	0.91
3.5–4.0	32	1958	4.13	25.58	0.91
4.0–4.5	37	1953	4.26	15.89	0.93
4.5–5.0	41	1949	4.10	13.53	0.93
5.0–5.5	45	1945	3.74	n.m.	n.m.
5.5–6.0	50	1940	3.65	22.73	0.92
6.0–6.5	54	1936	3.65	11.25	0.92
6.5–7.0	58	1932	3.69	17.49	0.91
7.0–7.5	63	1928	3.90	28.73	0.91
7.5–8.0	67	1923	3.71	13.34	0.92
8.0–8.5	71	1919	3.99	25.34	0.91
8.5–9.0	75	1915	3.81	17.35	0.92
9.0–9.5	80	1910	3.85	15.69	0.92
9.5–10.0	84	1906	3.64	12.24	0.91
10.0–10.5	88	1902	3.45	9.35	0.91
10.5–11.0	93	1897	3.73	6.97	0.91
11.0–11.5	97	1893	3.44	10.89	0.91
11.5–12.0	101	1889	3.37	8.01	0.91
12.0–12.5	106	1884	3.39	8.80	0.90
12.5–13.0	110	1880	3.49	10.57	0.91
13.0–13.5	114	1876	3.45	10.10	0.91
13.5–14.0	119	1871	3.74	10.50	0.91
14.0–14.5	123	1867	3.46	10.79	0.95
14.5–15.0	127	1863	3.21	11.69	0.90
15.0–15.5	131	1859	3.75	14.52	0.89
15.5–16.0	136	1854	4.77	14.96	0.91
16.0–16.5	140	1850	4.19	12.90	0.92
16.5–17.0	144	1846	3.81	11.08	0.89
17.0–17.5	149	1841	3.83	14.24	0.90
17.5–18.0	153	1837	3.51	12.24	0.88
18.0–18.5	157	1833	3.71	11.87	0.90
18.5–19.0	162	1828	3.99	10.95	0.90
19.0–19.5	166	1824	4.05	12.09	0.91
19.5–20.0	170	1820	4.28	18.78	0.89
20.0–20.5	175	1815	4.24	12.60	0.90
20.5–21.0	179	1811	3.97	14.00	0.90
21.0–21.5	183	1807	3.79	14.50	0.90
21.5–22.0	188	1803	3.47	17.76	0.90
22.0–22.5	192	1798	3.58	15.91	0.88
22.5–23.0	196	1794	3.53	11.55	0.89
23.0–23.5	200	1790	3.45	11.98	0.86
23.5–24.0	205	1785	3.70	10.49	0.86
24.0–24.5	209	1781	3.24	9.12	0.87
24.5–25.0	213	1777	3.30	n.m.	n.m.
25.0–25.5	218	1772	3.84	n.m.	n.m.
25.5–26.0	222	1768	4.00	6.35	0.87
26.0–26.5	226	1764	4.03	8.38	0.87
26.5–27.0	231	1759	4.25	8.18	0.87
27.0–27.5	235	1755	3.85	8.18	0.83
27.5–28.0	239	1751	3.41	15.85	0.86
28.0–28.5	244	1746	3.46	6.85	0.87
28.5–29.0	248	1742	3.86	7.36	0.88
29.0–29.5	252	1738	3.88	8.57	0.88
29.5–30.0	256	1734	3.77	9.59	0.87
30.0–31.0	263	1727	3.38	7.99	0.86

Captions: ^a, mean age of sediment horizon determined from average sedimentation rate (1.16 mm/yr); ^b, estimated date of deposition based on age of horizon and date of collection (August, 1990).

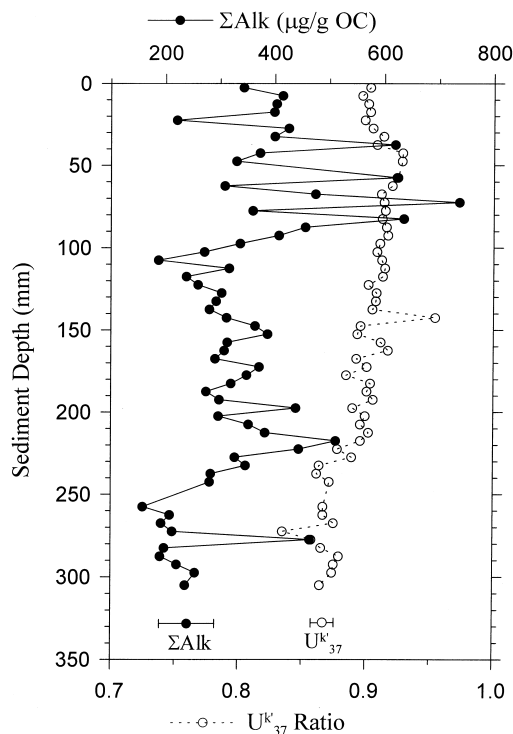


Fig. 5. Depth profiles of carbon-normalized total alkenone concentrations and $U_{37}^{K'}$ ratios for BC-43 sediments. The error bars for each measurement are illustrated at the bottom of the graph.

surface water temperatures in Guaymas Basin cannot be reconstructed accurately using a single linear relationship.

Several factors may contribute to the observed deviation from linearity between the $U_{37}^{K'}$ and SST. One factor to be considered is the physiological response of haptophyte algae at high ($>25^{\circ}\text{C}$) and low temperatures ($<5^{\circ}\text{C}$) ranges (e.g., Volkman et al., 1995). Recent work by Conte and co-workers (1998) clearly illustrates this effect, which results in nonlinear best fits between $U_{37}^{K'}$ ratio and temperature for different strains of *E. huxleyi* and *G. oceanica* (both of which are important species in the Gulf of California). A second factor that may contribute to the observed trends is the seasonal pattern in coccolithophore production in Guaymas Basin. The work of Ziveri and Thunell (2000) indicates that *E. huxleyi* dominates the flux during the spring and early summer (SSTs of $17\text{--}27^{\circ}\text{C}$) whereas *G. oceanica* is predominant during the late summer and early fall (SSTs of $28\text{--}32^{\circ}\text{C}$). Hence, changes in the species composition of alkenone producers also may contribute to the shift in response observed in the sediment trap samples at high temperatures (Fig. 6). Finally, it is possible that during periods of high SSTs, when there is a strong thermal stratification in the euphotic zone (e.g., Fig. 2), a significant fraction of alkenone producers may not inhabit the sea surface and therefore record lower-than expected temperatures in their $U_{37}^{K'}$ ratio (Ohkouchi et al., 1999). The chlorophyll distributions observed in the late summer and fall throughout the Gulf (e.g., Fig. 7) support this explanation. In this respect, it is important to note that the temperature differences between the sea surface and the subsurface chlorophyll maximum exhibited in Figure 7 are similar in magnitude to the offset observed between our data and the

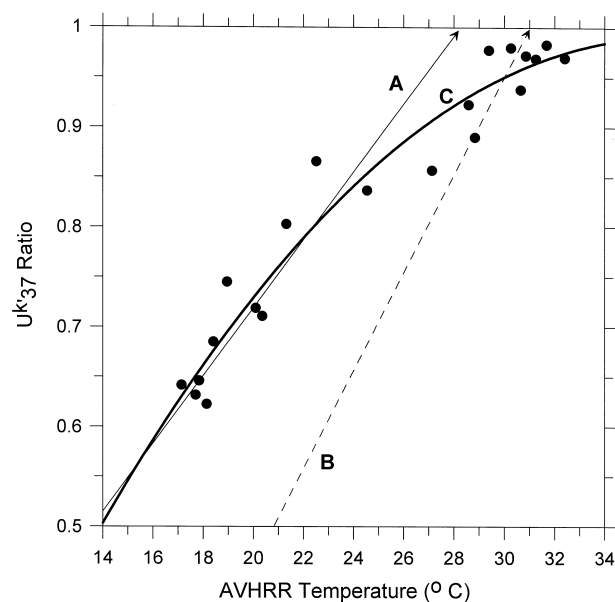


Fig. 6. Plot of AVHRR temperature vs. $U_{37}^{K'}$ ratios for the sediment trap samples. Line A represents the expression derived by Prahl and co-workers (1988) from laboratory incubations of *E. huxleyi*, whereas line B describes the expression developed by Volkman and co-workers (1995) for *G. oceanica*. Line C represents the nonlinear fit to the data using a 3rd order polynomial expression described in the text.

Prahl et al. relationship (Fig. 6). Unfortunately, we lack additional information to further constrain the regions within the water column where most alkenone producers live throughout the year in Guaymas Basin.

The nonlinear empirical relationship between the $U_{37}^{K'}$ index from sinking particles and SSTs in Guaymas Basin is in marked contrast with the core-top calibration studies of Rosell-Mele et al. (1995) and Muller et al. (1998), which spanned a temperature range of 0 to 29°C . Our sediment trap data show a good agreement with the core-top calibrations in the 17 to 26°C SST range but deviate significantly at higher temperatures ($28\text{--}32^{\circ}\text{C}$). Because of the strong evidence (see previous discussion) that this deviation from linearity is caused by oceanographic phenomena, we chose to fit the data points with a relatively simple 3rd order polynomial expression (Line C in Fig. 6: $U_{37}^{K'} = -0.295 + 0.0706T - 0.000969T^2$; $r^2 = 0.94$). We stress that this expression is not a new “calibration equation”. Instead, it represents an empirical best fit, which in this case plots between two established laboratory calibrations for *E. huxleyi* and *G. oceanica* (Prahl et al., 1988; Volkman et al., 1995). The data plotted in Figure 6 between 24 and 28°C can also be interpreted as a “step-function” and fitted to a higher order polynomial. A 5th order polynomial equation (line not shown) captures this trend. However, this latter expression behaves erratically in the lower T ranges and was therefore not utilized. Although the fit of line C is not perfect, we conclude that given the recurrent annual trend in SSTs (Fig. 3), this expression is a good proxy for describing seasonal changes in temperature at Guaymas Basin. It should be clear, however, that the accuracy of longer-term reconstructions will depend highly on the historical changes of maximum alkenone

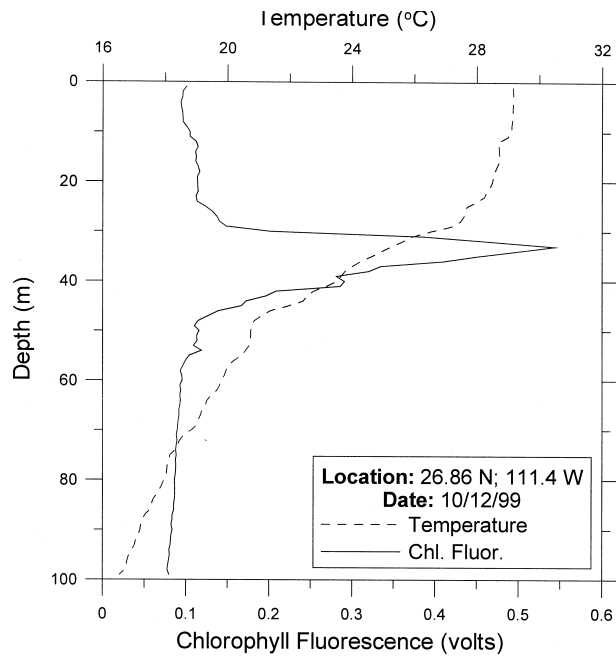


Fig. 7. Temperature and chlorophyll fluorescence profiles from a station in the central Gulf of California. The data were collected during the MOCE-5 cruise to the Gulf of California in October of 1999 by the Optical Oceanography Group at Oregon State University. The NASA SIMBIOS program funded this work.

flux, haptophyte species compositions, and thermocline structure.

6.2. Biogenic Fluxes in Guaymas Basin and Effects on $U_{37}^{K'}$ Signatures Recorded in Sediments

Total fluxes of alkenones were calculated by using the alkenone concentrations and the total mass flux data (Table 1). Total fluxes of opal, calcium carbonate and organic carbon were determined in a similar fashion (Thunell, 1998) and are plotted along with those for alkenones in Figure 8. Σ Alk fluxes, which range from 2.0 to 14 $\mu\text{g}/\text{m}^2/\text{day}$ (Fig. 8a), display a positive correlation with temperature ($r^2 = 0.5$). Σ Alk fluxes ($\leq 6 \mu\text{g}/\text{m}^2/\text{d}$) are generally low during the winter and early spring months, increasing in both 1996 and 1997 during the late spring and early summer as SSTs increase. High fluxes ($\geq 8 \mu\text{g}/\text{m}^2/\text{d}$) are measured during the summer and fall months, when the water column is highly stratified. Of all the major biogenic elements analyzed, calcium carbonate (Fig. 8b) is the only one which also shows a similar positive correlation ($r^2 = 0.3$) with temperature. For example, CaCO_3 fluxes decrease sharply from October 1996 to January of 1997 as active upwelling lowers SST and then increase again to maxima in May of 1997 as the thermocline develops. In contrast, marked maxima in opal fluxes occur during the initial and latter stages of upwelling (Fig. 8c), whereas OC fluxes show little or no relationship with SST (Fig. 8d). Visual examination of sedi-

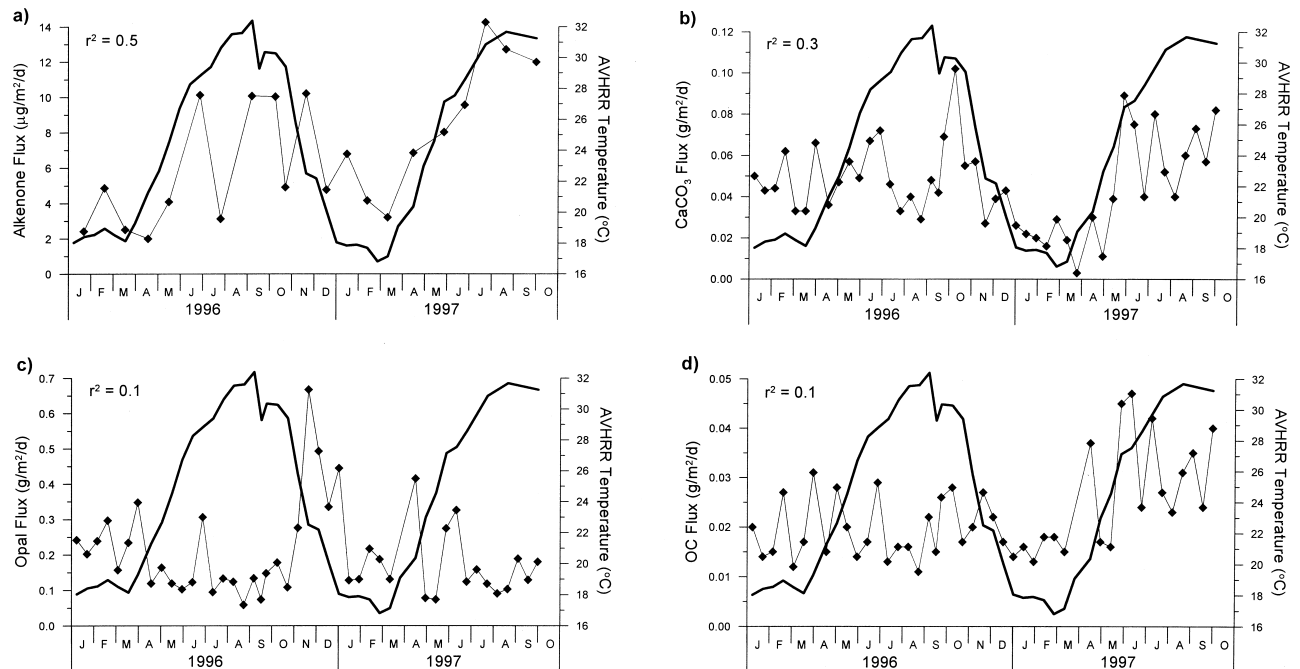


Fig. 8. Plots of a) total alkenone flux, b) calcium carbonate flux, c) opal flux, and d) organic carbon flux determined from the bi-weekly sediment trap samples for the 1996 through 1997 study period. Each graph also contains the AVHRR temperature record for the site (bold line). Details on the calculations of all of these parameters are discussed in the text. The alkenone and temperature data are tabulated in Table 1. Opal, organic carbon, and carbonate fluxes are from Thunell (1998). The correlation coefficient (r^2) between each flux and SST is indicated in each plot.

Table 4. Summary of alkenone fluxes and temperatures.

Parameter	Sediment traps		Core-top 1988–90 (0–0.5 cm)
	1996 (Jan–Dec)	1997 (Jan–Oct)	
Annual [37:3 Me] Flux Rate (mg/m ² /y)	0.263	0.403	0.454
Annual [37:2 Me] Flux Rate (mg/m ² /y)	1.84	2.74	4.23
Cumulative U ₃₇ ^{K'} Ratio ^a	0.875	0.872	0.903
Average AVHRR Temperature (°C) ^b	24.6	24.7	23.9
Average U ₃₇ ^{K'} Temperature (°C) (this study) ^c	25.5	25.5	26.9
Average U ₃₇ ^{K'} Temperature (°C) (Prah et al., 1988) ^d	24.6	24.5	25.4

The annual flux rates for the traps were estimated by calculating daily alkenone fluxes based on concentrations (mg/g sed) and mass flux (g/m²) for each trap period and multiplying it by 365 d/yr. The annual flux rates from the core-top were calculated by multiplying the alkenone concentrations by the mass accumulation rate (290 g/m²/y), the latter of which was estimated based on the average sedimentation rate (0.116 cm/yr) and the bulk density (0.25 g/cm³) of the sediments. Captions:

^a U₃₇^{K'} ratios calculated from the total alkenone fluxes for each period.

^b average AVHRR satellite temperatures are from the periods during which the sediment trap and core-top samples were collected.

^c U₃₇^{K'} temperatures estimated using the expression ($U_{37}^{K'} = -0.295 + 0.0706T - 0.000969T^2$) derived from the sediment trap data (Fig. 6).

^d U₃₇^{K'} temperatures estimated by using the Prah et al. (1988) equation.

ment trap samples reveals that the opal flux in Guaymas Basin is dominated by diatom cells, whereas much of the carbonate flux collected at this site is because of coccolithophores (Thunell et al, 1996). Therefore, these flux trends are consistent with a seasonal evolution of the plankton community in which diatoms bloom during the upwelling period, when nutrients are injected into the euphotic zone, whereas haptophyte production dominates during the oligotrophic, thermally stratified, periods (Thunell, 1998). As previously mentioned, the coccolithophore productivity follows a seasonal species succession, with *E. huxleyi* dominating in the early stages of surface warming and *G. oceanica* becoming predominant later on as the thermocline develops fully (Ziveri and Thunell, 2000).

Under these dynamic conditions, the seasonal pattern of alkenone fluxes through the water column can play a key role in determining the U₃₇^{K'} signature preserved in the sedimentary record of Guaymas Basin. The timing of alkenone production (Fig. 8a) indicates that the annual U₃₇^{K'} signature preserved in the sediments is likely to be biased towards elevated ratios and, therefore, weighted towards summer temperatures. To estimate the magnitude of this effect, we calculated the annual fluxes of [37:2 Me] and [37:3 Me] ketones for 1996 and 1997, and computed the cumulative U₃₇^{K'} ratios for each of period (Table 4). Notably, although the total alkenone fluxes are different in the two years studied, the resulting unsaturation indexes are virtually identical. Overall, our data suggest that inter-annual variability in the timing of alkenone productivity and delivery to the sediments are critical variables that exert a primary control on the U₃₇^{K'} sedimentary record at this and other sites (e.g., Prah et al., 1993).

By using the U₃₇^{K'}-SST calibration equation developed from the sediment trap data (Fig. 6), we estimated the annual temperatures that should be recorded in the underlying sediments (Table 4). According to this calculation, the alkenone-based temperature estimates are ~1°C higher than the annually averaged AVHRR temperatures for both 1996 and 1997, and reflect our observation that alkenone production is not uniform throughout the year. The major consequence of this finding is that the SST estimates garnered from the sediments at this location are likely to be warmer than the mean surface temper-

atures of the overlying water column. For comparison, we also have included the temperature estimates obtained by applying the Prah et al. (1988) equation to the cumulative alkenone fluxes. Coincidentally, the resulting U₃₇^{K'} temperatures match the average SSTs very well even though the Prah et al. equation does not adequately describe the sediment trap trends (Fig. 6). Such fortuitous agreement results from the underestimation of the high summer temperatures by the Prah equation, which counteracts the warm bias due to the timing in haptophyte productivity.

6.3. Relationship Between Core-Top Alkenone Data and Water Column SST

Because we have satellite coverage of the Guaymas Basin for 1989 to 1990, we can directly compare the mean AVHRR SST (23.9°C; Fig. 3) with the U₃₇^{K'} temperature estimate (26.8°C) recorded in the underlying sediments deposited during this period (Table 4). Such comparison reveals that the U₃₇^{K'} derived temperature estimated using the empirical relationship in Figure 3 is 3°C higher than the average SST for this two-year period. As explained in the previous section, about 1°C of this difference is due to the seasonal patterns in alkenone flux. However, other processes occurring at the water/sediment interface must be responsible for the additional ~2°C discrepancy. Two possible explanations include the preferential alteration of the alkenone signature reaching the sediments during cold water seasons, and the lateral input of alkenones that reflect warmer temperatures. Evidence for significant diagenetic losses at the water interface is lacking given the similar overall carbon-normalized alkenone concentrations in both sediment trap and sediment samples (Figs. 4 and 5). Strong evidence for advective alkenone inputs (and against diagenesis) is the fact that alkenone fluxes estimated for the top 5 mm of the sediment are markedly higher than those measured at 500 m water depth in the traps (Table 4). Hence, most of the remaining discrepancy between core-top U₃₇^{K'} and AVHRR SST estimates is probably because of the advection of alkenones via near-bottom currents, an effect that has been documented in other continental margin areas (e.g., Thomsen et al., 1998).

Additional characterization of the temperature signature derived from “allochthonous” alkenones at this site is necessary to verify the magnitude of such an effect. The application of the Prah1 et al. (1988) equation to the core-top sediments yields a temperature estimate that is 1.5°C higher than the average SST for their deposition period (Table 4).

6.4. SST Record for the Last 300 Years in the Gulf of California

Paleotemperature reconstructions that utilize a single calibration equation to estimate SSTs from sedimentary $U_{37}^{K'}$ ratios carry the assumption that the relationship between the two parameters has remained constant through the study period. Such an assumption is often difficult to test independently. For this study, we have chosen to compare temperature estimates derived by using the often-applied Prah1 et al. (1988) equation, which underestimates modern SSTs in Guaymas Basin, with those calculated by using the empirical expression derived above. Evidence for the constancy of the Prah1 et al. equation is provided by the core-top calibration studies discussed previously (e.g., Muller et al., 1998; Herbert et al., 1998) even though, as also mentioned above, there are plenty of examples in which this equation does not adequately describe modern ocean temperatures. For the latter approach, we used the relationship developed from the sediment trap data (Fig. 6) and applied a -3°C correction to account for warm-biases associated with the seasonality of alkenone productivity ($\sim 1^{\circ}\text{C}$) and the occurrence of lateral inputs ($\sim 2^{\circ}\text{C}$). The assumption behind this approach is that the seasonal and lateral input biases have remained constant throughout the depositional period. However, we have no evidence to indicate that this is indeed the case.

The rationale behind this exercise is our belief that, by investigating the differences between the temperature reconstructions derived from these two expressions, we may be able to determine whether or not the relationship between SSTs and $U_{37}^{K'}$ ratios has indeed varied with time. Furthermore, because factors such as variability in the timing and composition of haptophyte productivity and the lateral advection of “allochthonous” algal remain can affect the SST- $U_{37}^{K'}$ relationship, contrasts in the results obtained by using different expressions may also provide additional insights into past changes in oceanographic conditions. Finally, the estimates provided by the two expressions represent a range of reasonable past SSTs for the region that can be contrasted to other independent estimates of climate and oceanographic change.

Figure 9 shows the two temperature reconstructions based on the $U_{37}^{K'}$ ratios of box core sediments from BC-43 expanding approximately ~ 260 yr. Not surprisingly, given the previous discussion, there are significant differences between these two estimates. In fact, throughout most of BC-43, the Prah1 expression leads to SST estimates that are consistently 1 to 1.5°C higher than those obtained from the corrected empirical relationship (Fig. 9). Below 22 cm (ca. 1800), however, the difference between the two estimates widens to 2.5°C. The fact that this trend coincides with marked decreases in both temperature estimates suggests that the magnitude of the warm bias was lower in the 1700s than in more recent periods and may

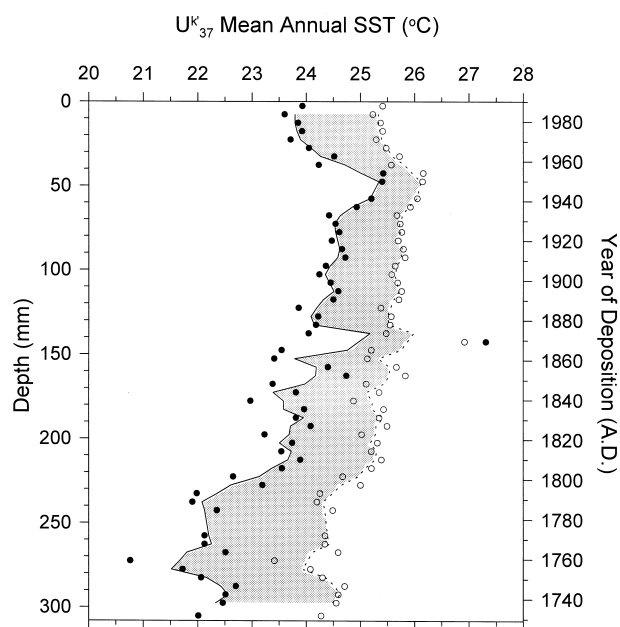


Fig. 9. Range of past sea surface temperatures reconstructed from the $U_{37}^{K'}$ signatures of sediments from BC-43. Closed symbols represent the estimates derived from Line C in Figure 6 after a -3°C correction (as explained in the text). The open symbols represent the temperature estimates derived by using the equation of Prah1 et al., 1988. The lines linking the data points represent 3-point moving averages. The age of each horizon were estimated from the accumulation rate and bulk density of the box core sediments (Table 2).

indicate a change in oceanographic conditions (e.g., productivity, lateral inputs).

Despite the variability in the estimates of absolute temperature yielded by the two different approaches, the data in Figure 9 suggest that a steady warming of over 2°C occurred in the surface waters of the Gulf of California from early 1700s to 1950. A more recent cooling of about 0.5 to 1°C follows this warming trend. The reasons for the progressive warming over the last three centuries are most likely associated with changes in solar irradiance (Lean et al., 1995) and increases in greenhouse gases (Mann et al., 1998). However, the warming we infer in the Gulf since the early 18th century is considerably larger than the $\sim 1.0^{\circ}\text{C}$ increase in global average temperature reported for this time period (Mann et al., 1998). The cooling in the latter half of the 20th century is more difficult to explain and may be related to processes, such as variations in the freshwater inputs to the Gulf or changes in deep-water formation rates, that decrease overall water column stratification. McCaffrey and co-workers (1990) also observed a similar recent cooling in a $U_{37}^{K'}$ record from the Peru margin. Without better temporal resolution and further studies, these explanations are merely speculative at this point.

7. SUMMARY

The overall objective of this study was to better understand the relationship between the $U_{37}^{K'}$ ratios of particulate organic matter and SSTs in an active upwelling region of the ocean. We analyzed the compositions of sediment trap samples to inves-

tigate the factors that contribute to the generation of the alkenone-based temperature proxy. These analyses revealed a highly linear relationship between $U_{37}^{K'}$ and SST during periods of relatively low temperature. In contrast, the $U_{37}^{K'}$ -SST relationship deviated significantly from linearity during periods when the water column was highly stratified and reached the highest temperatures. We conclude that several oceanographic processes are responsible to the observed nonlinear behavior of $U_{37}^{K'}$ parameter. One likely reason is the previously confirmed effect of high ($>25^{\circ}\text{C}$) temperatures on the alkenone biosynthesis by haptophyte algae (e.g., Volkman et al., 1995; Conte et al., 1998). Another important factor is the seasonal progression in alkenone producing haptophyte algae, from *E. huxleyi* to *G. oceanica*, that occurs during the spring and summer months in the gulf (Ziveri and Thunell, 2000). Finally, the possibility that alkenone producers may inhabit the subsurface during periods of high thermal stratification could also explain the lower-than-expected $U_{37}^{K'}$ ratios (Ohkouchi et al., 1999). Future efforts should focus on gaining a better understanding of how these and other oceanographic processes affect the generation and transport of the $U_{37}^{K'}$ signal through the water column. Specifically, the timing, location and species composition of alkenone production are areas that deserve additional attention.

We used the sediment trap flux data to evaluate the effect of seasonal changes in alkenone production on the annual $U_{37}^{K'}$ values recorded in surface sediments. Additionally, core-top sediments were used to constrain additional potential "biases" of $U_{37}^{K'}$ during deposition and burial. These investigations indicate that the $U_{37}^{K'}$ temperature signal preserved in Guaymas Basin sediments is $\sim 3^{\circ}\text{C}$ higher than expected. This discrepancy is in part because of the elevated alkenone fluxes during warm periods, which causes an overestimation of 1°C . The lateral input of alkenones from shallower region is thought to contribute an additional $\sim 2^{\circ}\text{C}$ to this effect. Importantly, our findings indicate that these warm biases are not caused simply by the preferential degradation of the 37:3 alkenone vs. its 37:2 counterpart (i.e., diagenetic effect) but are instead the result of factors such as the timing and origin of haptophyte productivity and alkenone fluxes.

Based on this improved understanding of the oceanographic processes that affect $U_{37}^{K'}$ as a temperature-proxy in this region, we produced a ~ 300 yr record of SST for the Gulf of California. A gradual 2°C warming from the early 1700s to the 1950s followed by a 1°C cooling in the last 40 yr is evident from the box core record. Further work should be carried out in this and other oceanographic regions to evaluate how the seasonal and annual changes in oceanographic conditions affect the preservation of the $U_{37}^{K'}$ -SST signal. It is imperative that we gain a better understanding of the mechanisms responsible for the alkenone compositions preserved in margin sediments before we can quantitatively assess the high-resolution records obtained from these regions of the oceans.

Acknowledgments—The crews of the RV El Puma and RV BIP are thanked for their assistance in the collection of samples. We would also like to thank Antoni Rosell-Mele for providing alkenone standards and Scott Pegau (from the Optical Oceanography Group at Oregon State University) for providing the CTD and chlorophyll data illustrated in Figure 7. This paper benefited from insightful reviews by Fred Prahl and Tim Herbert. We particularly would like to thank Fred Prahl for his constructive criticisms and energetic discussion. This research was

funded by NSF Grants OCE-9701940 and OCE-9711822 to M.G. and OCE-9301413 to R.T.

REFERENCES

- Alvarez-Borrego S. and Lara-Lara J. R. (1991) The physical environment and primary productivity of the Gulf of California. In *The Gulf and Peninsular Province of the Californias. American Association of Petroleum Geologists Memoir*, (ed. J. P. Dauphin and B. Simoneit) Vol. 47, pp. 555–567, American Association of Petroleum Geologists, Tulsa, OK, United States.
- Alvarez-Borrego S. S. and Schwartlose R. A. (1979) Water masses of the Gulf of California. *Ciencias Marinas* **6**, 43–63.
- Badan-Dangon A., Koblinsky C. J., and Baumgartner T. (1985) Surface thermal patterns in the Gulf of California. *Oceanologica Acta* **8**, 13–22.
- Badan-Dangon A. D., Clive E., Merrifield A., and Winant C. D. (1991) The lower atmosphere over the Gulf of California. *J. Geophys. Res.* **96**, 16877–16896.
- Baumgartner T. R., Ferreira-Bartrina V., and Moreno-Hentz P. (1991) Varve formation in the central Gulf of California: A reconsideration of the origin of the dark laminae from the 20th century varve record. In *The Gulf and Peninsular Province of the Californias. American Association of Petroleum Geologists Memoir*, (ed. J. P. Dauphin and B. Simoneit) Vol. 47, pp. 617–635.
- Bernal P. A. (1981) A review of the low frequency response to the pelagic ecosystem in the California current. *California Cooperative Oceanic Fisheries Investigations Report* **22**, 49–62.
- Brassell S. C., Eglinton G., Marlowe I. T., Pflaummann U., and Sarnthein M. (1986) Molecular stratigraphy: A new tool for climatic assessment. *Nature* **320**, 129–133.
- Bray N. A. (1988) Thermohaline circulation in the Gulf of California. *J. Geophys. Res.* **93**, 4993–5020.
- Calvert S. E. (1966) Origin of diatom-rich, varved sediments from the Gulf of California. *J. Geol.* **76**, 546–565.
- Conte M. H., Thompson A., Lesley D., and Harris R. P. (1998) Genetic and physiological influences on the alkenone/alkenoate versus growth temperature relationship in *Emiliania huxleyi* and *Gephyrocapsa oceanica*. *Geochim. Cosmochim. Acta* **62**, 51–68.
- Cutshall N. H., Larsen I. L., and Olsen C. R. (1983) Direct analyses of ^{210}Pb in sediment samples: Self-adsorption corrections. *Nuclear Instrument Methods* **206**, 309–312.
- Eglinton T., Conte M., Eglinton G., and Hayes J. (2000) Alkenone biomarkers gain recognition as molecular paleoceanographic proxies. *EOS, Transactions, American Geophysical Union* **81**, p. 253, 260.
- Epstein B. L., D'Hondt S., Quinn J. G., Zhang J., and Hargraves P. E. (1998) An effect of dissolved nutrient concentrations on alkenone-based temperature estimates. *Paleoceanography* **13**, 122–126.
- Froelich P. N. (1980) Analysis of organic carbon in marine sediments. *Limnology and Oceanography* **25**, 565–572.
- Goñi M. A., Ruttenger K. C., and Eglinton T. I. (1998) A reassessment of the sources and importance of land-derived organic matter in surface sediments from the Gulf of Mexico. *Geochim. Cosmochim. Acta* **62**, 3055–3075.
- Hartz D. M. (1998) Alkenones as indicators of past sea surface temperature in the Gulf of California. M.S. thesis, Univ. of South Carolina.
- Herbert T. D., Schuffert J. D., Thomas D., Lange C., Weinheimer A., Peleo-Alampay A., and Herguera J.-C. (1998) Depth and seasonality of alkenone production along the California margin inferred from a core top transect. *Paleoceanography* **13**(3), 263–271.
- Hoefs M. J. L., Versteegh G. J. M., Rijpstra W. I. C., de Leeuw J. D., and Damste J. S. S. (1998) Postdepositional oxic degradation of alkenones: Implications for the measurements of palae sea surface temperatures. *Paleoceanography* **13**, 42–49.
- Ikehara M., Kawamura K., Ohkouchi N., Kimoto K., Murayama M., Nakamura T., Oba T., and Taira A. (1997) Alkenone sea surface temperature in the Southern Ocean for the last two deglaciations. *Geophys. Res. Lett.* **24**, 679–682.
- Lean J., Beer J., and Bradley R. (1995) Reconstruction of solar irradiance since 1610: Implications for climate change. *Geophys. Res. Lett.* **22**, 3195–3198.

- Mann M., Bradley R., and Hughes M. (1998) Global-scale temperature patterns and climate forcing over the past six centuries. *Nature* **392**, 779–787.
- Marlowe I. T., Brassell S. C., Eglinton G., and Green J. C. (1984) Long chain unsaturated ketones and esters in living algae and marine sediments. *Organic Geochem.* **6**, 135–141.
- Marlowe I. T., Brassell S. C., Eglinton G., and Green J. C. (1990) Long-chain alkenones and alkyl alkenoates and the fossil coccolith record of marine sediments. *Chem. Geol.* **88**, 349–375.
- McCaffrey M. A., Farrington J. W., and Repeta D. J. (1990) The organic geochemistry of Peru margin surface sediments: I. A comparison of the C37 alkenone and historical El Niño records. *Geochim. Cosmochim. Acta* **54**, 1671–1682.
- Muller P. J., Kirst G., Ruhland G., von Storch I., and Rosell-Mele A. (1998) Calibration of the alkenone paleotemperature index UK'37 based on core-tops from the eastern South Atlantic and the global ocean (60° N–60°S). *Geochim. Cosmochim. Acta* **62**, 1757–1772.
- Ohkouchi N., Kawamura K., Kawahata H., and Okada H. (1999) Depth ranges of alkenone production in the central Pacific Ocean. *Global Biogeochemical Cycles* **13**, 695–704.
- Pelejero C. and Grimalt J. O. (1997) The correlation between the Uk37 index and sea surface temperature in the warm boundary: The South China Sea. *Geochim. Cosmochim. Acta* **61**, 4789–4797.
- Pelejero C., Grimalt J. O., Sarnthein M., Wang L., and Flores J.-A. (1999) Molecular biomarker record of sea surface temperature and climatic change in the South China Sea during the last 140,000 years. *Marine Geol.* **156**, 109–121.
- Prahl F. G., Collier R. B., Dymond J., Lyle M., and Sparrow M. A. (1993) A biomarker perspective on prymnesiophyte productivity in the northeast Pacific Ocean. *Deep-Sea Res.* **1** **40**, 2061–2076.
- Prahl R. G., Delange G. J., Lyle M., and Sparrow M. A. (1989) Post-depositional stability of long-chain alkenones under contrasting redox conditions. *Nature* **341**, 434–437.
- Prahl F. G., Muelhausen L. A., and Zahnle D. A. (1988) Further evaluation of long-chain alkenones as indicators of paleoceanographic conditions. *Geochim. Cosmochim. Acta* **52**, 2303–2310.
- Prahl F. G., Piasias N. G., Sparrow M. A., and Sabin A. (1995) Assessment of sea-surface temperature at 42°N in the California Current over the last 30,000 years. *Paleoceanography* **10**, 763–773.
- Prahl F. G. and Wakeham S. G. (1987) Calibration of unsaturation patterns in long-chain ketone compositions for palaeotemperature assessment. *Nature* **330**, 367–369.
- Pride C. (1997) An evaluation and application of paleoceanographic proxies in the Gulf of California. Ph.D. dissertation, Univ. of South Carolina.
- Robinson M. (1973) Atlas of monthly mean sea surface and subsurface temperatures in the Gulf of California. *San Diego Soc. Nat. Hist. Mem.* **5**, 1–97.
- Rontani J.-F., Cuny P., Grossi V., and Beker B. (1997) Stability of long-chain alkenones in senescing cells of *Emiliania huxleyi*: Effect of photochemical and aerobic microbial degradation on the alkenone unsaturation ratio (UK'37). *Organic Geochem.* **26**, 503–509.
- Rosell-Mele A., Carter J., Parry A. T., and Eglinton G. (1995a) Determination of the UK'37 index in geological samples. *Anal. Chem.* **67**, 1283–1289.
- Rosell-Mele A., Eglinton G., Pflaumann U., and Sarnthein M. (1995b) Atlantic core-top calibration of the Uk37 index as a sea-surface palaeotemperature indicator. *Geochim. Cosmochim. Acta* **59**, 3099–3107.
- Rosell-Mele A., Maslin M. A., Maxwell J. R., and Schaeffer P. (1997) Biomarker evidence for “Heinrich” events. *Geochim. Cosmochim. Acta* **61**, 1671–1678.
- Santamaria-del-Angel E., Alvarez-Borrego S., and Muller-Karger F. (1994) The 1982–1983 El Niño in the Gulf of California as seen in coastal zone scanner imagery. *J. Geophys. Res.* **99**, 7423–7431.
- Sikes E. L., Farrington J. W., and Keigwin L. D. (1991) Use of the alkenone unsaturation ratio Uk37 to determine past sea surface temperatures; core-top SST calibrations and methodology considerations. *Earth and Planetary Sci. Lett.* **104**, 36–47.
- Sikes E. L. and Keigwin L. D. (1994) Equatorial Atlantic sea surface temperature for the last 30 kyr; a comparison of Uk'37, delta 18O and foraminiferal assemblage temperature estimates. *Paleoceanography* **9**, 31–45.
- Sikes E. L. and Volkman J. K. (1993) Calibration of alkenone unsaturation ratios (Uk'37) for paleotemperature estimation in cold polar waters. *Geochim. Cosmochim. Acta* **57**, 1883–1889.
- Sikes E. L., Volkman J. K., Robertson L. G., and Pichon J.-J. (1997) Alkenones and alkenes in surface waters and sediments of the Southern Ocean: Implications for paleotemperature estimation in polar region. *Geochim. Cosmochim. Acta* **61**, 1495–1505.
- Sonzogni C., Bard E., and Rostek F. (1998) Tropical sea-surface temperatures during the last glacial period; a view based on alkenones in Indian Ocean sediments. *Quaternary Sci. Rev.* **17**, 1185–1201.
- Sonzogni C., Bard E., Rostek F., Dollfus D., Rosell-Mele A., and Eglinton G. (1997) Temperature and salinity effects on alkenone ratios measured in surface sediments from the Indian Ocean. *Quaternary Res.* **47**, 344–355.
- Teece M. A., Getliff J. M., Leftley J. W., Parkes R. J., and Maxwell J. R. (1998) Microbial degradation of the marine prymnesiophyte *Emiliania huxleyi* under oxic and anoxic conditions as model for early diagenesis; long chain alkenones, alkenones and alkyl alkenoates. *Organic Geochem.* **29**, 863–880.
- Ternois Y., Sicre M.-A., Boireau A., Beaufort L., Miquel J.-C., and Jeandel C. (1998) Hydrocarbons, sterols and alkenones in sinking particle in the Indian Ocean sector of the Southern Ocean. *Org. Geochem.* **28**, 489–501.
- Thomsen C., Schulz-Bull D. E., Petrick G., and Duinker J. C. (1998) Seasonal variability of the long-chain alkenone flux and the effect on the Uk'37-index in the Norwegian Sea. *Organic Geochem.* **28**, 311–323.
- Thunell R. C. (1998) Seasonal and annual variability in particle fluxes in the Gulf of California: A response to climate forcing. *Deep-Sea Res.* **1** **45**, 2059–2083.
- Thunell R. C., Pride C. J., Tappa E., and Muller-Karger F. E. (1993) Varve formation in the Gulf of California: Insights from time series sediment trap sampling and remote sensing. *Quaternary Sci. Rev.* **12**, 451–464.
- Thunell R. C., Pride C. J., Tappa E., and Muller-Karger F. E. (1994) Biogenic silica fluxes and accumulation rates in the Gulf of California. *Geology* **22**, 303–306.
- Thunell R. C., Pride C., Ziveri P., Muller-Karger F., Sancetta C., and Murray D. (1996) Plankton response to physical forcing in the Gulf of California. *J. Plankton Res.* **18**, 2017–2026.
- Villanueva J., Grimalt J. O., Cortijo E., Vidal L., and Labeyrie L. (1998) Assessment of sea surface temperature variations in the central North Atlantic using the alkenone unsaturation index (Uk37). *Geochim. Cosmochim. Acta* **62**, 2421–2427.
- Volkman J. K., Barrett S. M., Blackburn S. I., and Sikes E. L. (1995) Alkenones in *Gephyrocapsa oceanica*: Implications for studies of paleoclimate. *Geochim. Cosmochim. Acta* **59**, 513–520.
- Volkman J. K., Eglinton G., Corner E. D. S., and Forsberg T. E. V. (1980) Long-chain alkenes and alkenones in the marine coccolithophorid *Emiliania huxleyi*. *Phytochemistry* **19**, 2619–2622.
- Zeitzschel B. (1969) Primary productivity in the Gulf of California. *Marine Biol.* **3**, 201–207.
- Ziveri P. and Thunell R. (2000) Coccolithophore export production in Guaymas Basin, Gulf of California: Response to climate forcing. *Deep-Sea Res. Part II* **47**, 2073–2100.